ACS APPLIED MATERIALS & INTERFACES

Research Article

www.acsami.org

Plain Poly(acrylic acid) Gated Organic Field-Effect Transistors on a Flexible Substrate

Liviu M. Dumitru, Kyriaki Manoli, Maria Magliulo, Luigia Sabbatini, Gerardo Palazzo, and Luisa Torsi*

Department of Chemistry, "Aldo Moro" University, Via Orabona 4, Bari 70126, Italy

ABSTRACT: We report on the use of a polyanionic proton conductor, poly(acrylic acid), to gate a poly[2,5-bis(3-tetradecylthiophen-2-yl)thieno[3,2-*b*]thiophene]-based organic field-effect transistor (OFET). A planar configuration of the OFET is evaluated, and the electrical performance and implementation on a flexible substrate are discussed.

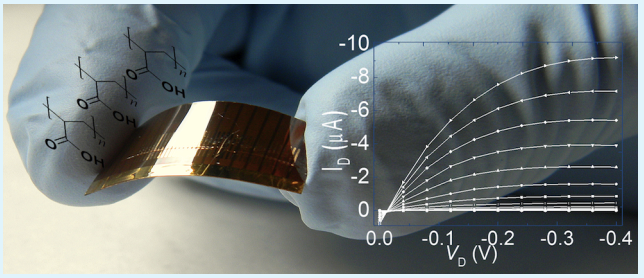

KEYWORDS: *electrolyte-gated organic thin-film transistors (OFETs), Debye−Helmholtz double layer, low-voltage operation, poly(acrylic acid), flexible electronics*

INTRODUCTION

Organic field-effect transistors (OFETs) have been widely investigated in the last years because of their potential use in low-cost, large-area, flexible electronic applications. OFETs fabricated on flexible substrates are indeed devices that can replace traditional "rigid" silicon-based electronics in areas where electronic devices, being lightweight, mechanically flexible, and fabricated by means of simple fabrication steps, are required.[1] Nowadays, several examples of OFETs holding these properties can be found.[2−6] Products such as electronic paper[7,8] and memory devices, including radio-frequency identification tags[9,10] and sensors,[11−14] are just a few of the high-impact OFET applications.

In an OFET structure, a dielectric between the thin organic semiconductor (OSC) layer and the gate electrode is needed to capacitively induce charges at the interface between the OSC and dielectric itself, and different chemical systems, such as inorganic oxides,[15] polymers,[16] or an ultrathin self-assembled monolayer,[17] have been proposed. Among the others, polymeric dielectrics are promising candidates for the fabrication of flexible electronic devices because they can combine high-*k* and conformability. Because most of the envisaged practical applications of organic electronics will require devices able to operate at low voltages, approaches such as increasing the effective capacitance of the gate dielectric (C_i)[18] by using high-*k* materials[19] and/or by decreasing its thickness (as demonstrated, for instance, in metal oxide layers such as TiO_2[20]) can be found.

An interesting alternative is the use of an electrolyte interface to gate an OFET, exploiting the Debye−Helmholtz double-layer high capacitance.[21] This is not a new concept because studies in which an electrolyte was employed to modulate the surface potentials of a germanium semiconductor were already proposed 60 years ago at Bell Labs.[22] Unless exploited on purpose and in controlled conditions, such as, for example, in electrochemically gated transistors,[23] one of the drawbacks of this approach is the occurrence, upon gate biasing, of ion penetration into the OSC layer.[24−26] The presence of ions inside the OSC can lead to undesired effects such as increases of the gate leakage and off-current, very low switching speed, and high hysteresis. This inconvenience can be overcome by using polyelectrolyte films composed of large anions that are almost immobile because of their steric hindrance. This occurrence prevents OSC doping when the OFET is operated in accumulation mode. In the case of polyelectrolyte-gated transistors, the electrical double layer (EDL) is formed at the semiconductor/polyelectrolyte interface[27] with an associated ion charge separation occurring upon application of a gate bias. Polyelectrolyte films can exhibit very high capacitance values (20−500 μF cm^{-2})[28,29] because of the small distance of a few angstroms existing between the charged sheets.[30] The large capacitance of these materials allows one to induce high carrier densities (~10^{15} charges cm^{-2})[31] in the OSC that exhibits a high current throughput at voltages lower than 1 V.[28,32] Even though the polarization mechanisms of electrolyte media under the gating potential are not yet fully understood, electrolyte-gated OFETs (EGOFETs) can exhibit very good performances and hold promise for low-cost printed organic electronics also because their fabrication procedures are compatible with solution-processed printing techniques. Several research groups have investigated and reported on the use of various polymer electrolytes[33,34] such as poly(ethylene oxide)-containing lithium salts (PEO/$LiClO_4$), cross-linked poly(acrylic acid) (PAA), and polyelectrolytes[28] such as poly(styrenesulfonic acid) as gating layers in OFETs. These devices are all capable of fulfilling the low-voltage operation requirement.

Received: July 24, 2013
Accepted: October 21, 2013
Published: October 21, 2013

OFET fabrication can involve spin coating of water-soluble polyelectrolytes directly onto the OSC surface because OSCs are usually insoluble in water. To reduce the ion mobility, polyelectrolytes can be cross-linked or copolymerized. However, the actual degrees of free ionic charges, as well as the whole polyelectrolyte bulk and interface capacitances, are usually difficult to quantify. Typical electrical parameters for a poly(3-hexylthiophene-2,5-diyl) (P3HT) OSC gated by a vinylphosphonic acid and acrylic acid P(VPA−AA) random copolymer have a threshold voltage (V_T) of −0.29 V and a field-effect mobility μ = 0.012 cm^2 V^{-1} s^{-1}.[31] Also interesting are the recently proposed electrolyte-gated OFETs for biosensing applications.[35−38]

In the cases of the polyelectrolyte-gated OFETs reported so far, both the OSC and gating layer were processed from solution, but the gating layer required either copolymerization[32] or a cross-linking[34] step. These procedures were considered necessary in order to minimize the cationic drift along with the connected p-type OSC electrochemical doping. Conventional PAA has already been identified as a performing gating material,[34] but a cross-linking step was considered necessary in order to minimize the gate leakage current and enhance the OFET on/off current ratio. On the other hand, the treatment resulted in a lowering of the polyelectrolyte conductivity, and good field-effect transistor $I-V$ curves were obtained by only biasing the device up to −20 V. A pristine, not annealed, PAA film is indeed an interesting, printable material that holds an ionic conductivity, at room temperature, in the range of 10^{-5} S cm^{-1} [22] and a high double-layer capacitance in the few microfaraday per square centimeter range.[39] This solid polyelectrolyte has also been used as a biocompatible[40] substrate for protein immobilization,[41] with this being of interest for future use in biosensing applications.

In this work, we reported the use of a polyanionic proton conductor, the plain PAA (Figure 1a), to gate a poly[2,5-bis(3-tetradecylthiophen-2-yl)thieno[3,2-*b*]thiophene], also known as the pBTTT-C14 (Figure 1b) OFET. The polyelectrolyte film and OSC are both deposited from solution. Compared to other solution-processable OSCs such as P3HT, for instance, pBTTT-C14 exhibits a higher field-effect mobility (with values as high as 1 cm^2 V^{-1} s^{-1})[42] thanks to its backbone rigidity and good crystalline order and is considered more stable.[43]

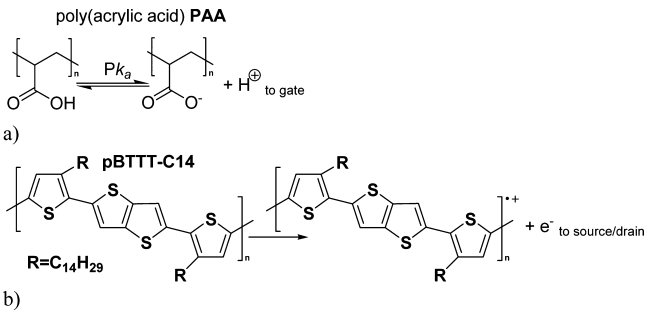

Figure 1. (a) Chemical structure of PAA protonated (left) and deprotonated (right). (b) Chemical structure of the pBTTT-C14 OSC in both its neutral (left) and doped (right) forms.

The PAA layer was processed from a water solution and drop-casted on top of the pBTTT-C14 layer in its pristine form without the need, for the first time to the best of our knowledge, for any cross-linking, annealing,[34] or blending step.[32]

EXPERIMENTAL SECTION

Materials. Poly(acrylic acid) (PAA; 35% w/v in water) and 1,2-dichlorobenzene were purchased from Sigma-Aldrich. The OSC poly[2,5-bis(3-tetradecylthiophen-2-yl)thieno[3,2-*b*]thiophene] (pBTTT-C14; electronic grade) was purchased from Ossila Ltd. and used as received. The flexible Kapton polyimide films were purchased from DuPont.

Device Fabrication. The PAA-gated transistors were fabricated by spin coating a pBTTT-C14 solution. The 30 nm OSC layer was spin-coated from a pBTTT-C14/1,2-dichlorobenzene (5 mg/mL) solution at 3000 rpm for 1 min on a flexible Kapton substrate. The flexible substrates was previously rinsed with acetone and deionized water; gold source (S) and drain (D) electrodes, defining a channel length (L) of 200 μm and a channel width (W) of 4000 μm, were patterned afterward. The S and D contacts are realized by means of gold thermal evaporation through a stainless steel shadow mask. The gate (G) electrode is thermally evaporated in the same step, perpendicular to the S and D electrodes as a gold strip (see Figure 2 for details).

To avoid an electrical shortcut between the OSC and gate contact, the gate itself, as well as the area between this contact and the S and D electrodes, was cleaned with 1,2-dichlorobenzene prior deposition of the PAA layer. After this, the pBTTT-C14 film was annealed at 110 °C for 1 min on a ceramic hot plate. The device was completed by drop-casting with a customized Doctor Blade deposition technique the proton conductor PAA viscous solution on top of the gate electrode and OSC. A stainless steel mask was used to define the area to be covered by the plain PAA. The device was left to dry at room temperature afterward.

Electrical Characterization. The current−voltage ($I-V$) characteristics were measured using a semiconductor parameter analyzer (Agilent 4155 C). The transfer characteristics (I_D vs V_G) were recorded, keeping the drain voltage (V_D) constant at −0.4 V. The transistor electrical parameters, namely, the field-effect mobility (μ), threshold voltage (V_T), and on/off current ratio (I_{on}/I_{off}), were extracted from the characteristic curves in the saturation regime. All measurements were carried out in ambient air (relative humidity ca. 36%; T = 25 °C).

RESULTS AND DISCUSSION

Because the capacitance of the layer is determined by the EDL confined at the polyelectrolyte/OSC interface, the polyelectrolyte layer thickness does not need to be strictly controlled.[44] Besides, because the polyelectrolyte is conductive, also the position of the gate is irrelevant.[32] These allow for an extremely simple fabrication procedure of a flexible OFET with a planar gate architecture.[45,46]

Upon application of a negative voltage to the gate electrode, the protons from the PAA layer accumulate to the negatively charged gate and form a Helmholtz layer at the PAA/gate electrode interface. A second double layer is formed at the interface between the deprotonated PAA immobile anions and the p-type pBTTT-C14 layer. The two-dimensional layer of positive charges accumulated in the OSC acts as the electronic channel of the transistor. Typical output and transfer characteristic curves of the PAA-gated pBTTT-C14 OFET are given in parts a and b of Figure 3, respectively.

The output characteristics show significant current modulation at a source−drain voltage (V_D) lower than −0.4 V, with this being among the lowest source and drain bias reported so far for an OFET. The maximum saturation current (I_D^{sat} = −9.18 μA) was measured also for a low applied gate voltage (V_G = −1 V) and can be directly associated with the large capacitance of the EDL formed at the polarized PAA/OSC interface. The red curve is the leakage current I_G, showing that a slight electrochemical doping is indeed present in the device.

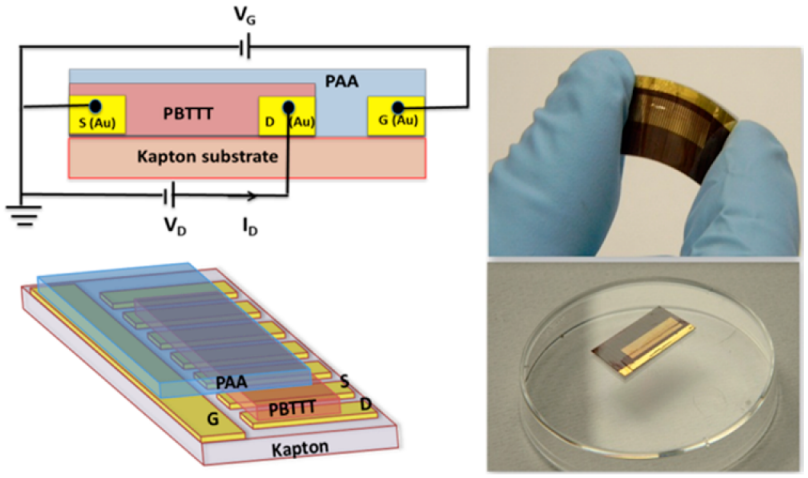

Figure 2. Schematic illustration and cross-sectional view of a PAA-gated OFET (left). Picture of a flexible PAA/pBTTT-C14-based OFET (right).

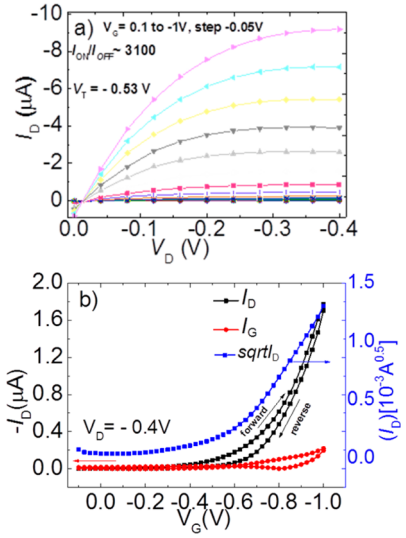

Figure 3. (a) PAA-gated pBTTT-C14 OFET output characteristics and (b) transfer curves. The black squares are the double-run plot of I_D versus V_G, while the red circles indicate the gate leakage; the blue squares are $I_D^{1/2}$ versus V_G. All data are taken at a fixed drain voltage of $V_D = -0.4$ V.

The current in the saturation regime (I_D^{sat}) follows the well-known equation[47,48]

$$I_D^{sat} = \frac{W}{2L}\mu C_i(V_G - V_T)^2 \quad (1)$$

where C_i is the capacitance per unit area of the gate insulator, μ is the charge-carrier field-effect mobility, and V_T is the threshold voltage. The transfer characteristics (Figure 3b) reveal the actual linear trend of $I_D^{1/2}$ versus V_G, in agreement with eq 1 with a threshold voltage (V_T) as low as −0.53 V. The best measured on/off current ratio (I_{on}/I_{off}) is 3100, while an average of ca. 900 was computed over 10 different devices (data reported in Table 1).

Compared to the values for other pBTTT-C14-based transistors with different dielectrics,[15,42] (see Table 2), the on/off ratio measured in this work is lower. This can be ascribed to a partial electrochemical doping of the OSC that has an impact on the off-current and on I_G, evaluated at zero source−drain bias, being about 10% of I_D^{sat}. Also, the hysteresis

Table 1. Electronic Performance Parameters (Field-Effect Mobility μ, Threshold Voltage V_T, and on/off Current Ratio) Extracted from the OFET $I-V$ Curves

pBTTT-C14-based OFET	average (n = 10)[a]	best
μ (cm^2 V^{-1} s^{-1})	0.55 ± 0.29	1.33
V_T (V)	−0.40 ± 0.05	−0.40
on/off	848 ± 889	3104

[a]Values are expressed as an average over 10 replicates, and errors are the relevant standard deviation.

observed in the transfer characteristics as well as in the I_D off-current can be associated with the electrochemical doping of the OSC. Indeed, the hygroscopic nature of the PAA layer can account for the fact that HO^- anions penetrate into the pBTTT-C14 matrix upon V_D and V_G negative bias. As a result, a current decrease in the reverse run can be expected because of the disorder induced at the interface caused by the ionic movement.

As was already anticipated, it is not always straightforward to measure the capacitance of the electrolyte systems. For this reason, the field-effect mobility (μ) is, at first, estimated from the slope (B) of the $I_D^{1/2}$ versus V_G plot (Figure 3b) using the equation

$$B = \sqrt{\frac{\mu C_i W}{2L}} \quad (2)$$

A comparison of the B parameter for OFETs similar to the pBTTT-C14/PAA-gated ones studied here is reported in Table 2. Data relevant to OFETs involving a pBTTT-C14 OSC and a silicone dioxide[15,42] or a polyelectrolyte as the gating material,[49] can be found. For the sake of comparison, the data relevant to P3HT[32] and pentacene[34] OFETs using a PAA-based gating material are reported also.

It is well-known that pBTTT-C14 and pentacene OSCs can exhibit field-effect transistor mobilities as high as 1 cm^2 V^{-1} s^{-1}, while that of P3HT is at least 1 order of magnitude lower. As can be seen, the value obtained for the B slope of the device presented in this work is higher than that extracted for the SiO_2-based ones. It is also clear that the B value extracted in the present study is higher than the one calculated for the chemically cross-linked PAA OFETs.[34]

An estimate of the device field-effect mobility can also be made by taking the polyelectrolyte double-layer capacitance as

Table 2. Comparison of the Electrical Performances of the Already Published pBTTT-C14-Based Transistors and PAA Dielectrics with Those of the OFET Studied in This Work

OSC	insulating/gating material	μ ($cm^2 V^{-1} s^{-1}$)	V_D (V)	V_G (V)	C_i ($F cm^{-2}$)	V_T (V)	slope B ($A V^{-2} cm^{-3}$)	I_{on}/I_{off}	ref
pBTTT-C14	SiO_2 (230 nm)	0.72	0 to −60	0 to −60	1.46×10^{-8}	9	0.0014	10^6	15
pBTTT-C14	SiO_2 (200 nm)	0.96	0 to −60	0 to −60	1.7×10^{-8}	∼9	0.0013	10^8	42
Pentacene	PAA chemically cross-linked	0.53	0 to −20	0 to −20	7.0×10^{-9}	−4.1	0.0000012	10^5	34
Pentacene	PAA thermally cross-linked	0.08	0 to −20	0 to −20	1.1×10^{-9}	−7.7	0.000054	10^4	34
P3HT	P(VPA−AA)	0.012	0 to −1.0	0 to −1.0	2.0×10^{-5}	−0.29	0.0016	10^2	32
pBTTT-C14	PAA	1.33[a]	0 to −0.4	0 to −1.0	N/A	−0.5	0.0062	10^3	this work

[a]PAA C_i taken from ref 39.

$C_i \sim 5.8$ μF cm^{-2}.[39] The highest mobility derived is $\mu \sim 1.33$ $cm^2 V^{-1} s^{-1}$, while the average over 10 replicates is 0.55 ± 0.29 $cm^2 V^{-1} s^{-1}$, which is comparable, within error, to that of the pBTTT-C14 SiO_2-gated devices.[15,42] A comparison can also be proposed with an electrochemical transistor using the same OSC, namely, pBTTT-C14.[49] Although the two devices rely on different gating mechanisms, it is interesting to note that a comparable mobility of 3.5 $cm^2 V^{-1} s^{-1}$ is reported for the electrochemical one by assuming a double-layer capacitance of 100 μF cm^{-2} and extracting the mobility from a three-dimensional charge-density model.

CONCLUSIONS

In conclusion, we report the use of a pristine, bare polyanionic proton conductor to gate an OFET fabricated on flexible Kapton substrates. The novelty of this work resides in the fact that no polymerization or cross-linking steps were used before casting of the polyelectrolyte and no annealing step was necessary either. A planar configuration was used to fabricate the devices, thus making the patterning of the source, drain, and gate electrodes very simple and attractive because it requires only one step. Low electrochemical doping of the OSC was observed, and the electronic performances of the devices are comparable to those reported for other pBTTT-C14-based OFETs, with the difference being that the devices proposed here can be operated at voltages lower than −0.4 V.

AUTHOR INFORMATION

Corresponding Author

*E-mail: luisa.torsi@uniba.it.

Notes

The authors declare no competing financial interest.

ACKNOWLEDGMENTS

The "Gas sensor on flexible substrates for wireless applications−FlexSmell" project, SEVENT FRAMEWORK PROGRAMME FP7-People-ITN-2008 under Grant 238454, is acknowledged for financial support of this work. Prof. Krishna Persaud and Ehsan Danesh from the University of Manchester are acknowledged for useful discussions. This work was partially supported by PRIN 2010-2011 Project 2010BJ23MN Nanostructured Soft Matter: from Fundamental Research to Novel Applications and by CSGI.

REFERENCES

(1) Cho, J. H.; Lee, J.; Xia, Y.; Kim, B. S.; He, Y.; Renn, M. J.; Lodge, T. P.; Frisbie, C. D. *Nat. Mater.* **2008**, *7*, 900−906.
(2) Kim, D.; Lee, S. H.; Jeong, S.; Moon, J. *Electrochem. Solid-State Lett.* **2009**, *12*, 195−197.
(3) Loi, A.; Manunza, I.; Bonfiglio, A. *Appl. Phys. Lett.* **2005**, *86*, 103512−103515.
(4) Wang, C. H.; Hsieh, C. Y.; Hwang, J. C. *Adv. Mater.* **2011**, *23*, 1630−1634.
(5) Cho, H.; Yoon, H.; Char, K.; Hong, Y.; Lee, C. *Jpn. J. Appl. Phys.* **2010**, *49*, 05EB08.
(6) Jedaa, A.; Halik, M. *Appl. Phys. Lett.* **2009**, *95*, 103309−103312.
(7) Rogers, J. A.; Bao, Z.; Baldwin, K.; Dodabalapur, A.; Crone, B.; Raju, V.; Kuck, V.; Katz, H.; Amundson, K.; Ewing, J. *Proc. Natl. Acad. Sci. U.S.A.* **2001**, *98*, 4835−4840.
(8) Gelinck, G. H.; Huitema, H. E. A.; van Veenendaal, E.; Cantatore, E.; Schrijnemakers, L.; van der Putten, J. B. P. H.; Geuns, T. C. T.; Beenhakkers, M.; Giesbers, J. B.; Huisman, B. H. *Nat. Mater.* **2004**, *3*, 106−110.
(9) Voss, D. *Nature* **2000**, *407*, 442−444.
(10) Baude, P.; Ender, D.; Haase, M.; Kelley, T.; Muyres, D.; Theiss, S. *Appl. Phys. Lett.* **2003**, *82*, 3964−3966.
(11) Lin, P.; Luo, X.; Hsing, I.; Yan, F. *Adv. Mater.* **2011**, *23*, 4035−4040.
(12) Angione, M. D.; Cotrone, S.; Magliulo, M.; Mallardi, A.; Altamura, D.; Giannini, C.; Cioffi, N.; Sabbatini, L.; Fratini, E.; Baglioni, P. *Proc. Natl. Acad. Sci. U.S.A.* **2012**, *109*, 6429−6434.
(13) Yang, S. Y.; Cicoira, F.; Byrne, R.; Benito-Lopez, F.; Diamond, D.; Owens, R. M.; Malliaras, G. G. *Chem. Commun.* **2010**, *46*, 7972−7974.
(14) Huang, W. G.; Besar, K.; LeCover, R.; Rule, A. M.; Breysse, P. N.; Katz, H. E. *J. Am. Chem. Soc.* **2012**, *134*, 14650−14653.
(15) McCulloch, I.; Heeney, M.; Bailey, C.; Genevicius, K.; MacDonald, I.; Shkunov, M.; Sparrowe, D.; Tierney, S.; Wagner, R.; Zhang, W. *Nat. Mater.* **2006**, *5*, 328−333.
(16) Parashkov, R.; Becker, E.; Ginev, G.; Riedl, T.; Johannes, H. H.; Kowalsky, W. *J. Appl. Phys.* **2004**, *95*, 1594−1596.
(17) Halik, M.; Klauk, H.; Zschieschang, U.; Schmid, G.; Dehm, C.; Schutz, M.; Maisch, S.; Effenberger, F.; Brunnbauer, M.; Stellacci, F. *Nature* **2004**, *431*, 963−966.
(18) Facchetti, A.; Yoon, M. H.; Marks, T. J. *Adv. Mater.* **2005**, *17*, 1705−1725.
(19) Roberts, M. E.; Mannsfeld, S. C. B.; Querlato, N.; Reese, C.; Locklin, J.; Knoll, W.; Bao, Z. *Proc. Natl. Acad. Sci. U.S.A.* **2008**, *105*, 12134−12134.
(20) Majewski, L. A.; Schroeder, R.; Grell, M. *Adv. Funct. Mater.* **2005**, *15*, 1017−1022.
(21) Kim, S. H.; Hong, K.; Xie, W.; Hyung Lee, K.; Zhang, S.; Lodge, T. P.; Frisbie, C. D. *Adv. Mater.* **2012**, *25*, 1822−1840.
(22) Brattain, W. H.; Garrett, C. G. B. *Bell Syst. Tech. J.* **1955**, *34*, 129−176.
(23) Khodagholy, D.; Curto, V. F.; Fraser, K. J.; Gurfinkel, M.; Byrnw, R.; Diamond, D.; Malliaras, G. G.; Benito-Lopez, F.; Owens, R. M. *J. Mater. Chem.* **2012**, *22*, 4440−4443.
(24) Yuen, J. D.; Dhoot, A. S.; Namdas, E. B.; Coates, N. E.; Heeney, M.; McCulloch, I.; Moses, D.; Heeger, A. J. *J. Am. Chem. Soc.* **2007**, *129*, 14367−14371.
(25) Kaake, L.; Zou, Y.; Panzer, M.; Frisbie, C.; Zhu, X. *J. Am. Chem. Soc.* **2007**, *129*, 7824−7830.

(26) Lee, J.; Kaake, L. G.; Cho, J. H.; Zhu, X. Y.; Lodge, T. P.; Frisbie, C. D. *J. Phys. Chem. C* **2009**, *113*, 8972−8981.
(27) Lee, J.; Panzer, M. J.; He, Y.; Lodge, T. P.; Frisbie, C. D. *J. Am. Chem. Soc* **2007**, *129*, 4532−4533.
(28) Said, E.; Crispin, X.; Herlogsson, L.; Elhag, S.; Robinson, N. D.; Berggren, M. *Appl. Phys. Lett.* **2006**, *89*, 143507−143510.
(29) Mitra, S.; Shukla, A.; Sampath, S. *J. Power Sources* **2001**, *101*, 213−218.
(30) Grahame, D. C. *Chem. Rev.* **1947**, *41*, 441−501.
(31) Panzer, M. J.; Frisbie, C. D. *Adv. Funct. Mater.* **2006**, *16*, 1051−1056.
(32) Herlogsson, L.; Crispin, X.; Robinson, N. D.; Sandberg, M.; Hagel, O. J.; Gustafsson, G.; Berggren, M. *Adv. Mater.* **2007**, *19*, 97−101.
(33) Panzer, M. J.; Newman, C. R.; Frisbie, C. D. *Appl. Phys. Lett.* **2005**, *86*, 103503−103506.
(34) Lim, S. H.; Kim, J.; Lee, S.; Kim, Y. S. *Chem. Commun.* **2010**, *46*, 3961−3963.
(35) Cotrone, S.; Ambrico, M.; Toss, H.; Angione, M. D.; Magliulo, M.; Mallardi, A.; Berggren, M.; Palazzo, G.; Horowitz, G.; Ligonzo, T.; Torsi, L. *Org. Electron.* **2012**, *13*, 638−644.
(36) Kergoat, L.; Piro, B.; Berggren, M.; Pham, M.-C.; Yassar, A.; Horowitz, G. *Org. Electron.* **2012**, *13*, 1−6.
(37) Buth, F.; Kumar, D.; Stutzmann, M.; Garrido, J. A. *Appl. Phys. Lett.* **2011**, *98*, 153302−153305.
(38) Haeberle, T.; Munzer, A. M.; Buth, F.; GArrido, J. A.; Abdellah, A.; Fabel, B.; Luigi, P.; Scarpa, G. *Appl. Phys. Lett.* **2012**, *101*, 223101−223106.
(39) Parsonage, E. E. *J. Colloid Interface Sci.* **1996**, *177*, 353−358.
(40) De Giglio, E.; Cometa, S.; Cioffi, N.; Torsi, L.; Sabbatini, L. *Anal. Bioanal. Chem.* **2007**, *389*, 2055−2063.
(41) Hollmann, O.; Czeslik, C. *Langmuir* **2006**, *22*, 3300−3305.
(42) Hamadani, B.; Gundlach, D.; McCulloch, I.; Heeney, M. *Appl. Phys. Lett.* **2007**, *91*, 243512−243515.
(43) Umeda, T.; Kumaki, D.; Tokito, S. *J. Appl. Phys.* **2009**, *105*, 024516−024521.
(44) Lee, K. H.; Zhang, S.; Lodge, T. P.; Frisbie, C. D. *J. Phys. Chem. B* **2011**, *115*, 3315−3321.
(45) Dasgupta, S.; Stoesser, G.; Schweikert, N.; Hahn, R.; Dehm, S.; Kruk, R.; Hahn, H. *Adv. Funct. Mater.* **2012**, *22*, 4909−4919.
(46) Lee, S. W.; Kim, B. S; Park, J. J.; Hur, J. H.; Kim, J. M.; Sekitani, T.; Someya, T.; Jeong, U. *J. Mater. Chem.* **2011**, *21*, 18804−18809.
(47) Braga, D.; Horowitz, G. *Adv. Mater.* **2009**, *21*, 1473−1486.
(48) Torsi, L.; Dodabalapur, A.; Heeney, M.; Lovinger, A. J.; Katz, H. E; Ruel, R.; Davis, D. D.; Baldwin, K. W. *Chem. Mater.* **1995**, *7*, 2247−2251.
(49) Dhoot, A. S.; Yuen, J. D.; Heeney, M.; McCulloch, I.; Moses, D.; Heeger, A. J. *Proc. Natl. Acad. Sci. U.S.A.* **2006**, *103*, 11834−11837.